Bull. Mater. Sci. (2019) 42:72
https://doi.org/10.1007/s12034-019-1756-x

Enhancement of ethanol-sensing properties of ZnO nanoplates by UV illumination

LUONG HUU PHUOC, DO DUC THO*, NGUYEN TIEN DUNG, VU XUAN HIEN, DANG DUC VUONG and NGUYEN DUC CHIEN
School of Engineering Physics, Hanoi University of Science and Technology, Hanoi 112 400, Vietnam
*Author for correspondence (tho.doduc@hust.edu.vn)

MS received 28 March 2018; accepted 5 September 2018; published online 6 March 2019

Abstract. ZnO nanoplates with hexagonal wurtzite structure were synthesized by hydrothermal treatment. The average dimension and average thickness of the plates were ~200 × 400 and 40 nm, respectively. ZnO nanoplates were deposited on Pt-interdigitated electrodes for the fabrication of gas-sensing devices. The ethanol-sensing properties of the devices were investigated in the dark *vs.* ultraviolet (UV) illumination. Under the UV illumination, the optimal operating temperature of the devices can be reduced from 237 to 164°C and the response of the device was increased from 2.8 to 8.5 towards 1500 ppm ethanol vapour.

Keywords. Hydrothermal; UV illumination; ZnO nanoplate; ethanol vapour sensing.

1. Introduction

In recent years, controlling and monitoring ethanol has become important in testing drunk drivers [1]. Indeed, prolonged heavy consumption of ethanol can cause significant permanent damage to the brain and other organs [2] and the enduring alcohol abuse becomes a major public health problem with major repercussions for individuals, the health care system and society, in general [3]. Hence, ethanol detection and monitoring is important. Among metal oxide semiconductors, zinc oxide (ZnO), a type II–VI semiconductor with a wide and direct band gap of 3.37 eV (at 300 K) and a large free exciton binding energy of 60 meV [1], is one of the most promising materials for gas sensors, especially for detecting ethanol vapour [1,4]. The sensor operation-based ZnO nanomaterial exhibits resistance change during the injection of target gas on the ZnO surface. The sensing properties of ZnO are directly related to its morphology and operating temperature [5]. Nevertheless, ZnO exhibits limitations, such as high operating temperature and poor sensitivity, which probably limit its applications. These drawbacks can be addressed by doping transition elements [6,7] and noble metals [8] or irradiation of ultraviolet (UV) light [9,10]. These approaches enhance the gas-sensing performance of the devices. In addition, UV illumination is a potential solution to reduce the working temperature.

For sensing enhancement using UV light activation, de Lacy Costello *et al* [11] showed that a sensor based on particulate ZnO activated with UV LED at a peak wavelength of 400 nm and incident light intensity of 2.2 mW cm^{-2} can detect very low concentrations of acetone and acetaldehyde (1 ppb). Zhai *et al* [12] revealed that C-doped ZnO exhibits excellent UV-activated room temperature gas-sensing activity at 500°C calcination for ethanol detection. These studies were conducted at room temperature. A recent study reported the influence of UV light combined with thermal energy on sensing materials [13–15]. However, research on this field is limited.

There are a variety of methods to synthesize ZnO nanoplates, such as thermal evaporation [16], electrochemical deposition [17], chemical-bath deposition [18], chemical-vapour deposition [19] and so on. However, these methods usually need high temperature, high pressure, high energy consumption and high cost. Hence, finding a simple, low cost and low energy consumption method to synthesize ZnO nanoplates is required.

In this paper, we report a free-catalysed synthesis of ZnO nanoplates by hydrothermal treatment without templates and activating surfactant agents. The ethanol-sensing properties of the ZnO nanoplates during the induction of UV light were investigated. The ethanol-sensing mechanism of the material under UV illumination at various temperatures was also proposed and discussed.

2. Experimental

ZnO nanoplates were synthesized by hydrothermal treatment at 180°C for 24 h using zinc nitrate hexahydrate ($Zn(NO_3)_2 \cdot 6H_2O$; 99%, China), potassium hydroxide (KOH; 85%, China) and absolute ethanol (99.6%, China) as starting materials. The procedure has been reported in ref. [15]. The crystal structure of ZnO nanoplates was identified using Bruker-AXS

(Siemens) D5005 with CuKα radiation ($\lambda = 1.54065$ Å) at a scanning rate of 0.03°/2 s within the 2θ range of 30–70°. The morphology of the nanopowder was identified by scanning electron microscopy (Nova nanoSEM 450).

For the gas-sensing measurement, the sensor device was prepared by the following procedure: at first, the obtained ZnO powder was dispersed with polyethylene glycol (PEG, 4000) into distilled water at room temperature, then placed onto Pt-interdigitated electrodes (the electrode gap is 20 µm) and spin coated at 1800 rpm for 60 s. The device was dried in air at 80°C for 24 h and heated at 600°C for 2 h to evaporate organic species. The sensor device was placed in a plate of external electric heater inside a glass chamber. A UV LED (wavelength, 365 nm; power, 1 W) was placed in the opposite direction above the device. The current–voltage (I–V) characteristic and ethanol-sensing performance of the device were determined using a static gas-sensing system. The response of the device towards 125–1500 ppm ethanol was tested at 100–300°C.

3. Results and discussion

High-density ZnO nanoplates with smooth surfaces were synthesized (figure 1a). The ZnO nanoplates exhibit regular shapes with an average size of 200 × 400 nm and thickness of ~40 nm. The typical XRD pattern of the nanoplates (figure 1b) depicts that all the diffraction peaks can be assigned to the hexagonal wurtzite of ZnO with lattice constants of $a = b = 0.3249$ and $c = 0.5206$ nm (JCPDS 36-1451). The strong and narrow diffraction peaks indicate that the material possesses good crystallinity. The crystallite size of the nanoplate is 24.8 nm, which is calculated for the most intense peak (101) by using the Scherrer equation [20]:

$$D = \frac{0.89\lambda}{\beta \cos\theta}, \tag{1}$$

where D is the crystallite size (nm), β the full width of the diffraction line at half of the maximum intensity i.e., (101) in radians, $\lambda = 1.54065$ Å the X-ray wavelength of CuKα and θ the Bragg's angle.

First, we tested the response of the ZnO nanoplate film to UV light by three cycles at 138°C (figure 2). For example, the dynamic response is stable and reproducible with a good on/off current ratio. The voltage on the film increases intensively under UV illumination. This effect can be attributed to the fact that UV light stimulates carrier generation and consequently increases the density of free electron–hole pairs in the ZnO film through the following reaction [14]:

$$h\nu \rightarrow \mathrm{h}^+ + \mathrm{e}^- \tag{2}$$

Figure 3 shows the I–V characteristics of the ZnO nanoplate film at various working temperatures in the dark (figure 3a) and under UV illumination (figure 3b). The I–V curves of the device under UV illumination display higher slope than

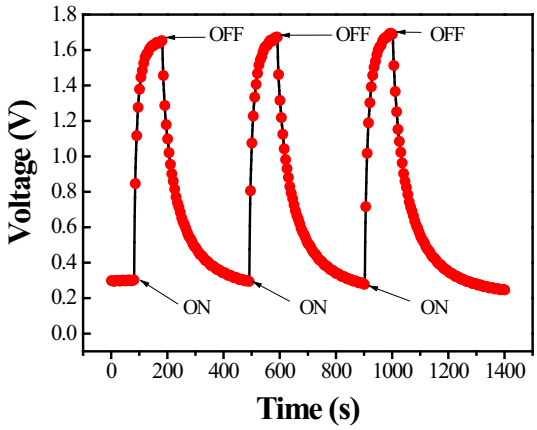

Figure 2. Response of ZnO nanoplates film to UV light at 138°C.

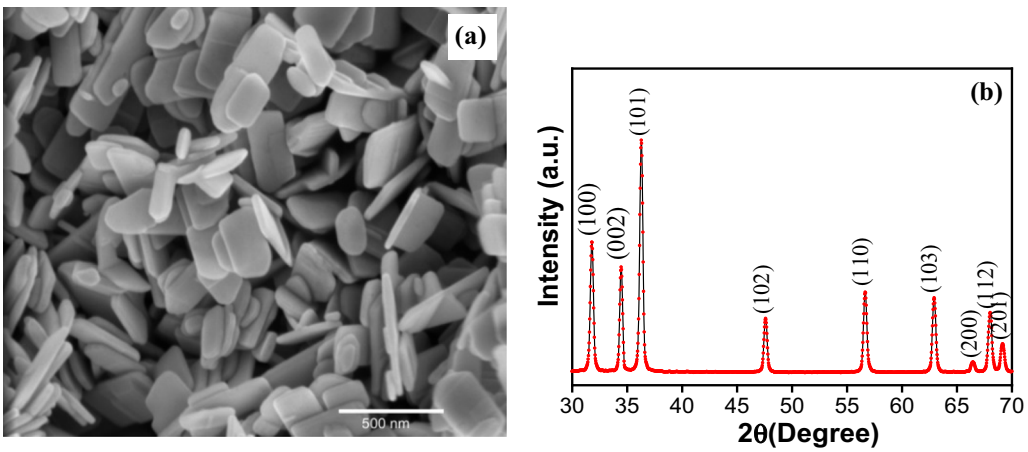

Figure 1. (**a**) SEM image and (**b**) XRD pattern of ZnO nanoplates.

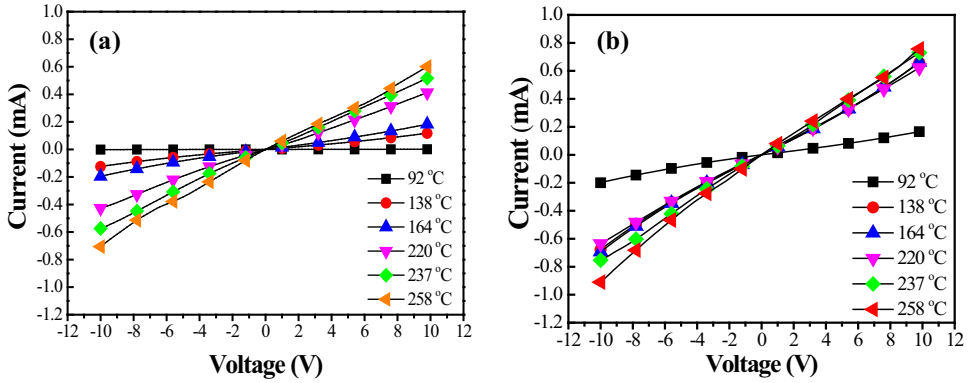

Figure 3. *I–V* characteristics of ZnO nanoplates film at differential working temperatures in the (**a**) dark and (**b**) under UV illumination.

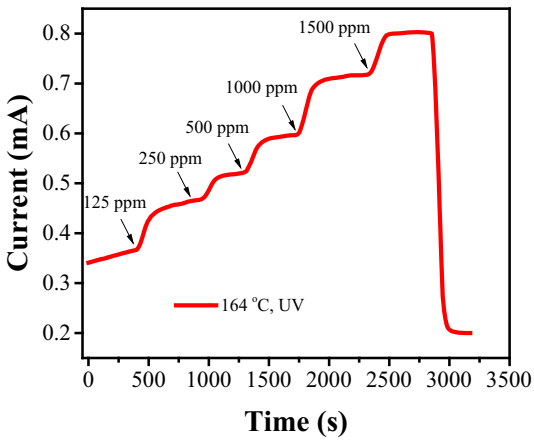

Figure 4. Transient response of ZnO nanoplate film to ethanol vapour (125–1500 ppm) under UV illumination at 164°C.

those of the device in the dark. This observation indicates that the resistance of the ZnO thin film decreases under UV illumination. In addition, the *I–V* curve at 92°C under UV illumination is less sloped than the ones in the dark.

The transient response of the ZnO nanoplate film shown in figure 4 depicts the influence of UV illumination on the sensitivity of sample at 164°C. The resistive curve is adequately clear. The response time for 125 ppm ethanol vapour is 154.4 s and the recovery time for 1500 ppm ethanol vapour is 114.2 s. Hence, we can observe that ethanol molecules are quickly desorbed on the film.

Figure 5 presents the response of the ZnO nanoplate film to ethanol vapour (125–1500 ppm) at various working temperatures in the dark (figure 5a) and under UV illumination (figure 5b). We observe that the film response reaches the maximal value at 237 and 164°C for all ethanol vapour concentration levels in the dark and under UV illumination, respectively. The film response to 1500 ppm ethanol vapour is 8.5 at 164°C under UV illumination and 2.8 at 237°C in the dark. This result indicates that under UV illumination, the optimal working temperature of the film decreases and the film response increases. Moreover, the response of the ZnO nanoplate to vapour ethanol can be determined at temperatures higher than 92°C under UV illumination. In the dark, the response can be determined only at temperatures higher than 164°C. A possible explanation is related to the

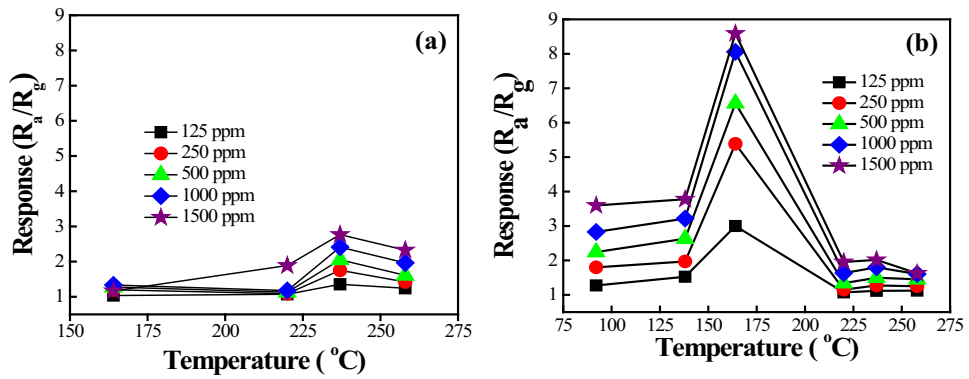

Figure 5. Responses of ZnO nanoplate film to ethanol vapour (125–1500 ppm) at various working temperatures in the (**a**) dark and (**b**) under UV illumination.

Table 1. List of light-activated ethanol sensors based on ZnO nanostructures.

Sensor material	Wavelength(nm)/energy (mW cm^{-2})	Working temperature (°C)	Ethanol (ppm)	Response	Reference
ZnO	365	350	400	—	[21]
Au–ZnO	254/4.1	125	1000	6.3; R_a/R_g	[22]
ZnO	Visible light	160	300	4.0; $[(C_g - C_a)/C_g^a]$	[23]
ZnO	365/4 W	60	500	75%; $[((R_a - R_b)/R_a) \times 100\%]$	[24]
ZnO	365	164	1000	8.0; R_a/R_g	This work

[a] C_a and C_g: the conductance of sensor in ambient air and in the presence of ethanol vapour, respectively.

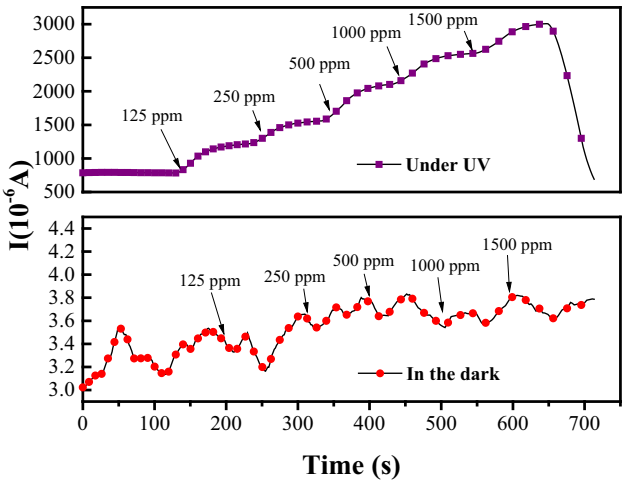

Figure 6. Transient response of ZnO nanoplate film to ethanol vapour (125–1500 ppm) at 138°C in the (**a**) dark and (**b**) under UV illumination.

photoconduction of the ZnO nanoplate that is affected due to oxygen adsorption under UV illumination.

The sensor response of the device in this work has been compared with the previously published reports as shown in table 1. It shows the high performance of sensor based on ZnO nanoplate under UV illumination when it was exposed towards ethanol vapour at low temperatures.

Figure 6 illustrates that the response of ZnO nanoplate film can be determined from the response curve at 138°C under UV illumination (figure 6b). Although the resistive curve is slightly unclear, the film response can be calculated. In the dark, the film shows no response to ethanol vapour at all concentration levels (figure 6a).

For ethanol gas-sensing, oxygen adsorption influences the electrical transport properties of ZnO nanoplates. On the surface of ZnO nanoplates, reactive oxygen ions, such as O_2^-, O^- and O^{2-}, are mainly chemisorbed with the aid of thermal energy in the dark. The reactions kinetics can be described as follows [25]:

$$O_{2,g} \leftrightarrow O_{2,ads}, \tag{3}$$

$$O_{2,ads} + e^- \leftrightarrow O_{2,ads}^-, \tag{4}$$

$$O_{2,ads}^- + e^- \leftrightarrow 2O_{ads}^-, \tag{5}$$

$$O_{ads}^- + e^- \leftrightarrow O_{lat}^{2-}, \tag{6}$$

where the subscripts 'g', 'ads' and 'lat' mean gas, adsorbed and lattice, respectively.

These oxygen ions react with ethanol vapour introduced into the glass chamber by the following reaction [25]:

$$C_2H_5OH_{ads} + 6O_{ads}^- \rightarrow 2CO_2 + 3H_2O + 6e^-. \tag{7}$$

These reactions release electrons back to the conduction band of ZnO which decrease the surface depletion layer width, and subsequently, increase the electrical conductivity of the sensor sample. Therefore, the film response evidently increases when the film is exposed to ethanol vapour.

Under UV illumination, the free electron–hole pairs could be generated by equation (2). Besides, the photoinduced hole may interact with chemisorbed oxygen ion, causing the oxygen to be desorbed from the ZnO film surface by equation [9]:

$$h^+ + O_{2,ads}^- \rightarrow O_{2,g}. \tag{8}$$

Photogenerated oxygen ions are created due to the reaction of ambient oxygen molecules with photoelectrons as follows [9]:

$$O_2 + e^-(h\nu) \rightarrow O_2^-[h\nu]. \tag{9}$$

In contrast to the chemisorbed oxygen ions, which are strongly attached to the ZnO surface, these photogenerated oxygen ions $O_2^-[h\nu]$ are weakly bound to ZnO and can be easily removed [10]. The ethanol molecules will react rapidly with these additional photogenerated oxygen ions on the ZnO surface according to the following equation [13,26]:

$$C_2H_5OH + 3O_2^-[h\nu] \rightarrow 2CO_2 + 3H_2O + 3e^-. \tag{10}$$

Hien *et al* [27] showed that the desorption of water molecules in the deep layers of the film appears at 164°C. As the places

which were occupied by water molecules can be exposed to UV irradiation. It could result in an increase in the amount of photogenerated oxygen ions and activating sites located in the film surface. In addition, it can also increase the amount of ethanol molecules which were available to interact directly with the surface. At higher temperatures, the amount of photogenerated oxygen ions and activating sites located in the film surface are probably maintained, but the desorption ratio of ethanol from film surface to air may increase, so the response of the film decreases. Hence, the sensitivity of the ZnO nanoplate film under UV illumination reaches the maximum at 164°C.

4. Conclusion

ZnO nanoplates with wurtzite structure and average thickness of 40 nm were successfully synthesized by a wet-chemical process through hydrothermal technique at 180°C for 20 h without templates and activating surfactant agents. UV illumination significantly enhances the sensitivity of ethanol vapour sensor based on ZnO nanoplates. Under UV illumination, the response of the film based on this material can reach a value of 8.5 at 164°C. In addition, illuminating the zinc oxide-based gas sensor with energy radiation can reduce the operating temperature of the sensor compared with the band gap of the metal oxide. The observed enhancement of ethanol sensing of film at low temperature is attributed to the influence of UV illumination. This sensor can be used in areas where working at high temperatures is unfeasible, thereby significantly enhancing its applicability.

Acknowledgement

This work was supported by the project code B2017-BKA-49.

References

[1] Mirabbaszadeh K and Mehrabian M 2012 *Phys. Scr.* **85** 035701
[2] Young S J, Lin Z D, Hsiao C H and Huang C S 2012 *Int. J. Electrochem. Sci.* **7** 11634
[3] Morey T E, Booth M M, Prather R A, Nixon S J, Boissoneault J, Melker R J *et al* 2011 *J. Anal. Toxicol*. **35** 134
[4] Wan Q, Li Q H, Chen Y J, Wang T H, He X L, Li J P *et al* 2004 *Appl. Phys. Lett.* **84** 3654
[5] Lupan O, Chai G and Chow L 2008 *Microelectron. Eng.* **85** 2220
[6] Shishiyanu S T, Shishiyanu T S and Lupan O I 2005 *Sens. Actuators B* **107** 379
[7] Koshizaki N and Oyama T 2000 *Sens. Actuators B* **66** 119
[8] Tien L C, Sadik P W, Norton D P, Voss L F, Pearton S J, Wang H T *et al* 2005 *Appl. Phys. Lett.* **87** 1
[9] Fan S W, Srivastava A K and Dravid V P 2009 *Appl. Phys. Lett.* **95** 10
[10] Lu G, Xu J, Sun J, Yu Y, Zhang Y and Liu F 2012 *Sens. Actuators B* **162** 82
[11] de Lacy Costello B P J, Ewen R J, Ratcliffe N M and Richards M 2008 *Sens. Actuators B* **134** 945
[12] Zhai J, Wang L, Wang D, Lin Y, He D and Xie T 2012 *Sens. Actuators B* **161** 292
[13] Zhang P, Pan G, Zhang B, Zhen J and Sun Y 2014 *Mater. Res.* **17** 817
[14] Dhahri R, Hjiri M, El Mir L, Bonavita A, Iannazzo D, Latino M *et al* 2016 *J. Phys. D: Appl. Phys.* **49** 135502
[15] Nguyen D D, Do D T, Vu X H, Dang D V and Nguyen D C 2016 *Adv. Nat. Sci. Nanosci. Nanotechnol.* **7** 015004
[16] Umar A and Hahn Y B 2006 *Nanotechnology* **17** 2174
[17] Illy B, Shollock B A, MacManus-Driscoll J L and Ryan M P 2005 *Nanotechnology* **16** 320
[18] Yuliarto B, Nulhakim L, Ramadhani M F, Iqbal M, Nugraha S and Nuruddin A 2015 *IEEE Sens. J.* **15** 4114
[19] Okazaki K, Nakamura D, Higashihata M, Iyamperumal P and Okada T 2011 *Opt. Express* **19** 20389
[20] Huang J, Dai Y, Gu C, Sun Y and Liu J 2013 *J. Alloys Compd.* **575** 115
[21] Zhu L, Li Y and Zeng W 2017 *Phys. E* **94** 123
[22] Wongrat E, Chanlek N, Chueaiarrom C, Samransuksamer B, Hongsith N and Choopun S. 2016 *Sens. Actuators A* **251** 188
[23] Wu B, Lin Z, Sheng M, Hou S and Xu J 2016 *Appl. Surf. Sci.* **360** 652
[24] Lin C H, Chang S J and Hsueh T J 2016 *Mater. Res. Express* **3** 1
[25] Karimi M, Ezzati M, Akbari S and Lejbini M B 2013 *Curr. Appl. Phys.* **13** 1758
[26] Chen Y, Li X, Li X, Wang J and Tang Z 2016 *Sens. Actuators B* **232** 158
[27] Hien V X, Lee J-H, Kim J-J and Heo Y-W 2014 *Sens. Actuators B* **194** 134